

Commensurate and incommensurate Haldane phases for a spin-1 bilinear-biquadratic model

Yan-Wei Dai(代艳伟), Ai-Min Chen(陈爱民), Xi-Jing Liu(刘希婧), and Yao-Heng Su(苏耀恒)
Citation: Chin. Phys. B, 2023, 32 (**9**): 090304. DOI: 10.1088/1674-1056/acac0c
Journal homepage: http://cpb.iphy.ac.cn; http://iopscience.iop.org/cpb

What follows is a list of articles you may be interested in

Degenerate polarization entangled photon source based on a single Ti-diffusion lithium niobate waveguide in a polarization Sagnac interferometer

Yu Sun(孙宇), Chang-Wei Sun(孙昌伟), Wei Zhou(周唯), Ran Yang(杨然), Jia-Chen Duan(端家晨), Yan-Xiao Gong(龚彦晓), Ping Xu(徐平), and Shi-Ning Zhu(祝世宁)
Chin. Phys. B, 2023, 32 (**8**): 080308. DOI: 10.1088/1674-1056/acd8b3

Algorithm for evaluating distance-based entanglement measures

Yixuan Hu(胡奕轩), Ye-Chao Liu(刘烨超), and Jiangwei Shang(尚江伟)
Chin. Phys. B, 2023, 32 (**8**): 080307. DOI: 10.1088/1674-1056/acd5c5

Improving source-in-the-middle continuous-variable quantum key distribution using a heralded hybrid linear amplifier

Lei-Xin Wu(伍磊鑫), Yan-Yan Feng(冯艳艳), and Jian Zhou(周健)
Chin. Phys. B, 2023, 32 (**7**): 070310. DOI: 10.1088/1674-1056/ac9b39

Faithful and efficient hyperentanglement purification for spatial-polarization-time-bin photon system

Fang-Fang Du(杜芳芳), Gang Fan(樊钢), Yi-Ming Wu(吴一鸣), and Bao-Cang Ren(任宝藏)
Chin. Phys. B, 2023, 32 (**6**): 060304. DOI: 10.1088/1674-1056/aca395

Review of quantum simulation based on Rydberg many-body system

Zheng-Yuan Zhang(张正源), Dong-Sheng Ding(丁冬生), and Bao-Sen Shi(史保森)
Chin. Phys. B, 2021, 30 (**2**): 020307. DOI: 10.1088/1674-1056/abd744

Commensurate and incommensurate Haldane phases for a spin-1 bilinear–biquadratic model

Yan-Wei Dai(代艳伟)[1,†], Ai-Min Chen(陈爱民)[2,‡], Xi-Jing Liu(刘希婧)[3], and Yao-Heng Su(苏耀恒)[2]

[1] *Centre for Modern Physics and Department of Physics, Chongqing University, Chongqing* 400044, *China*
[2] *School of Science, Xi'an Polytechnic University, Xi'an* 710048, *China*
[3] *The School of Materials Science and Engineering, Chongqing Jiaotong University, Chongqing* 400044, *China*

(Received 15 September 2022; revised manuscript received 17 November 2022; accepted manuscript online 16 December 2022)

Commensurate and incommensurate Haldane phases for a spin-1 bilinear-biquadratic model are investigated using an infinite matrix product state algorithm. The bipartite entanglement entropy can detect a transition point between the two phases. In both phases, the entanglement spectrum shows double degeneracy. We calculate the nonlocal order parameter of the bond-centered inversion in both phases, which rapidly approaches a saturation value of -1 as the segment length increases. The nonlocal order parameter of the bond-centered inversion with a saturation value -1 and the nonzero value string order indicate that the Haldane phase is a symmetry-protected topological phase. To distinguish the commensurate and incommensurate Haldane phases, the transversal spin correlation and corresponding momentum distribution of the structure factor are analyzed. As a result, the transversal spin correlations exhibit different decay forms in both phases.

Keywords: commensurate and incommensurate phases, symmetry-protected topological phase, transversal spin correlation

PACS: 03.67.–a, 03.67.Mn, 05.70.Fh, 75.40.Mg **DOI:** 10.1088/1674-1056/acac0c

1. Introduction

Quantum phase transitions are always a hot topic of interest in condensed matter physics, which are driven by quantum fluctuations due to the uncertainty principle in quantum mechanics. One of the targets is towards completing classification of quantum states of matter.[1] In 1983, Haldane[2,3] conjectured that the half-integer spin antiferromagnetic Heisenberg chain is gapless, and the integer spin chain has an energy gap between the ground state and the first excited state. For the spin-1 Heisenberg chain, a symmetry protected topological (SPT) phase, i.e., the Haldane phase, induces a long-range string order, due to the hidden symmetry of fully broken $Z_2 \times Z_2$. Interestingly, the Haldane phase in the spin-1 bilinear-biquadratic (BLBQ) model displays two parts in the structure of the Haldane phase,[4–7] i.e., the commensurate Haldane (Haldane$_{\rm C}$) phase and incommensurate Haldane (Haldane$_{\rm IC}$) phases.

Let us recall the ground state phase diagram of the spin-1 BLBQ model with the Hamiltonian described as

$$H = \sum_{j=1}^{\infty} \left[(\boldsymbol{S}_j \boldsymbol{S}_{j+1}) + \alpha (\boldsymbol{S}_j \boldsymbol{S}_{j+1})^2 \right], \tag{1}$$

where $\boldsymbol{S}_i$ denotes the spin-1 operator at lattice site i, and $\alpha = \tan\phi$ is the control parameter. The model has been investigated extensively using analytical and numerical methods,[8–20] exhibiting rich physics. Its ground state phase diagram has been mostly understood. At $\phi = 0$, the model corresponds to the spin-1 Heisenberg antiferromagnet, and for $\phi = \pi/4$, the model has been exactly solved by Sutherland,[21] who in turn justified the presence of the critical phase with central charge $c = 2$[20] for $\pi/4 \leq \phi < \pi/2$. The model exhibits SU(3) symmetry[22,23] at $\phi = \pm\pi/2$, $\pi/4$, and $-3\pi/4$, and a gapless ferromagnetic phase with a multi-fold degenerate is detected from $\phi = \pi/2$ to $\phi = -3\pi/4$. For $\phi = -\pi/2$ the model has been solved by Takhtajan and Bubujian,[24,25] which turns out to be the SU(2) WZW model at level $k = 2$, with the central charge $c = 3/2$. At $\phi = -\pi/4$, Barber and Batchelor[26] solve the model in terms of the Bethe ansatz, which indicates that the dimerized phase exists nearby. Whether or not the phase transition from the gapless ferromagnetic phase to the dimerized phase is direct remains controversial. However, this controversial problem has been solved in our previous work.[16] Reference [16] showed the absence of a critical nematic phase in the vicinity of an SU(3) ferromagnetic point ($\phi = -3\pi/4$) by means of tensor network algorithms. At the SU(3) ferromagnetic point $\phi = -3\pi/4$, the ground state wave function is highly degenerated, which is scaled but not conformally invariant, with the fractal dimension $d_{\rm f}$ being equal to 2. In addition, for $\phi = \arctan(1/3)$, the model has been exactly solved by Affleck, Kennedy, Lieb, and Tasaki (AKLT),[27] with its ground state being the valence-bond-solid state. For $-\pi/4 < \phi < \pi/4$, the model is in the gapped Haldane phase with hidden topological order;[3,28] the gapped Haldane phase can divide into two subphases (Haldane$_{\rm C}$ and Haldane$_{\rm IC}$) by

†Corresponding author. E-mail: daiyw@cqu.edu.cn
‡Corresponding author. E-mail: chenaimin_xa@163.com

© 2023 Chinese Physical Society and IOP Publishing Ltd

the AKLT point.

The transitions between commensurate and incommensurate are important problems in quantum many-body spin systems and are induced by frustration. Physically, "incommensurate" means that the wavelength of the oscillation pattern is not an integer multiple of the lattice spacing. Normally, it is not easy to characterize the incommensurate phase. Therefore, characterization of the commensurate and incommensurate phases is an important problem in physics. Here, we focus on the gapped Haldane phase for $-\pi/4 < \phi < \pi/4$. Murashima *et al.*[4] characterized the Haldane$_{\rm C}$–Haldane$_{\rm IC}$ change by analyzing the energy gap of edge states. Fáth *et al.*[5] proposed an effective field theory to explain these features in the Haldane$_{\rm C}$–Haldane$_{\rm IC}$ change of the spin-1 BLBQ chain. In addition, Nomura[6] proposed a mechanism to explain the onset of the incommensurability and the shortest correlation length at AKLT point and a simple random-walk-type argument is proposed to explain the Haldane$_{\rm C}$–Haldane$_{\rm IC}$ transition in Ref. [7]. Our characterization in this study is a numerical method from the tensor network in that we use the transversal spin correlations $\langle S^+S^-\rangle$ and the corresponding momentum distribution of the structure factor $S^{+-}(q)$ to characterize the Haldane$_{\rm C}$ and Haldane$_{\rm IC}$ phases. The transversal spin correlations $\langle S^+S^-\rangle$ exhibit different decay forms in both subphases. The results show that the transversal spin structure factor $S^{+-}(q)$ exhibits an incommensurate oscillation pattern in the Haldane$_{\rm IC}$. Our numerical method can provide a powerful tool for characterizing incommensurable phases. In addition, the transition point $\alpha_{\rm c}(\chi)$ between the Haldane$_{\rm C}$ and Haldane$_{\rm IC}$ phases is detected by using von Neumann entropy. The singular values of second-order derivatives of the von Neumann entropy correspond to the transition points $\alpha_{\rm c}(\chi)$. As a typical example of the SPT phase,[29–31] the Haldane phase is protected by any of the following three symmetries: bond-centered inversion symmetry, time-reversal symmetry, and a dihedral group comprising any pair of π-rotations in the spin space.[29,30] In order to further characterize the Haldane$_{\rm C}$ and Haldane$_{\rm IC}$ phases, we also calculate the nonlocal order parameter. The nonlocal order parameter of the bond-centered inversion with a saturation value of -1 and the nonzero value string order indicate that the Haldane phase is a symmetry-protected topological phase.

In this study, the infinite matrix product state (iMPS) algorithm[32] is used to calculate the ground state wave function with χ as the bond dimension. The remainder of this article is organized as follows. In Section 2, bipartite entanglement entropy and entanglement spectrum are calculated; a transition point is located between the Haldane$_{\rm C}$ and Haldane$_{\rm IC}$ phases, corresponding to the AKLT point with $\alpha = 1/3$. In Section 3, we discuss the bond-centered inversion nonlocal order parameter. Section 4 discusses the string order parameter, and Section 5 characterizes the Haldane$_{\rm C}$ and Haldane$_{\rm IC}$ phases using the transversal spin correlations $\langle S^+S^-\rangle$ and the corresponding momentum distribution of the structure factor $S^{+-}(q)$. Finally, a summary is presented in Section 6.

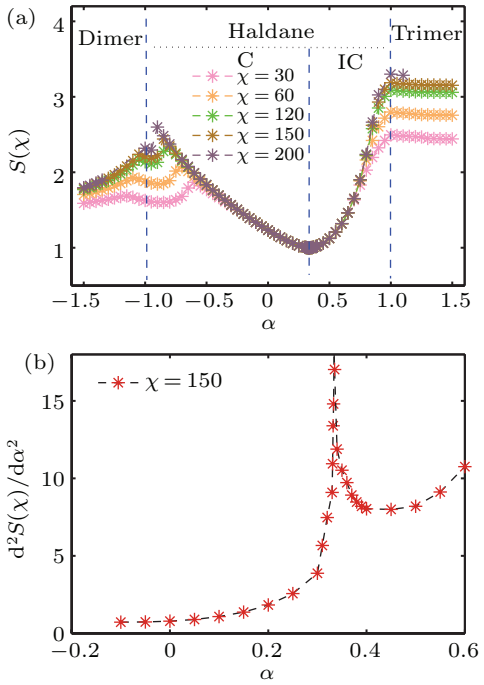


Fig. 1. (a) Bipartite entanglement entropy $S(\chi)$ as a function of the parameter α with bond dimensions $\chi = 30$, 60, 120, 150, and 200. (b) The second-order derivatives of the entanglement entropy $S(\chi)$ as a function of the parameter α. The bond dimension is $\chi = 150$.

2. Bipartite entanglement entropy and entanglement spectrum

The von Neumann entropy is a measure of bipartite entanglement for a quantum state, which is exploited to detect a transition point. This entropy is from the perspective of quantum information on the study phase transition. For a system of a pure state partitioned into two subsystems A and B, the bipartite entanglement entropy is defined as $S = -\mathrm{Tr}\rho_{\rm A}\log\rho_{\rm A} = -\mathrm{Tr}\rho_{\rm B}\log\rho_{\rm B}$, where $\rho_{\rm A} = |\psi_{\rm A}\rangle\langle\psi_{\rm A}|$ ($\rho_{\rm B} = |\psi_{\rm B}\rangle\langle\psi_{\rm B}|$) denotes the reduced density matrix of subsystem A (B). In this study, we obtain the ground state wave function $|\psi\rangle$ using the iMPS algorithm[32] from tensor network simulations. In the iMPS representation, the bipartite entanglement entropy for a semi-infinite chain may be rewritten as follows:

$$S(\chi) = -\sum_{v=1}^{\chi} \lambda_v^2 \log_2 \lambda_v^2, \tag{2}$$

where λ denotes the Schmidt decomposition coefficient, and χ denotes the bond dimension. Because we consider that the translation of two lattice points is invariant, entanglement entropy $S(\chi) = (S_{\rm a} + S_{\rm b})/2$. The bipartite entanglement entropy $S(\chi)$ is plotted in Fig. 1(a) as a function of the parameter α with the bond dimensions $\chi = 30$, 60, 120,150,

and 200. In the region $-1.5 \leq \alpha \leq 1.5$, three phase transition points are located at $\alpha = -1, 1/3, 1$ from the entanglement entropy, and they correspond to four phases: the dimerized phase, Haldane$_{\rm C}$ phase, Haldane$_{\rm IC}$ phase, and trimerized phase. Notably, an antiferromagnetic phase occurs between the dimerized phase and Haldane$_{\rm C}$ phases, which disappears as the bond dimension χ increases. In this study, we focus on the Haldane phase. To detect the transition point $\alpha_{\rm c}(\chi)$ between the Haldane$_{\rm C}$ and Haldane$_{\rm IC}$ phases, we plot the second-order derivatives of the entanglement entropy $S(\chi)$ as a function of the parameter α in Fig. 1(b), with the bond dimension $\chi = 150$. A singular point appears at the $\alpha = 0.334$, which is very close to the AKLT point $\alpha = 1/3$. Our results indicate a transition at the AKLT point.

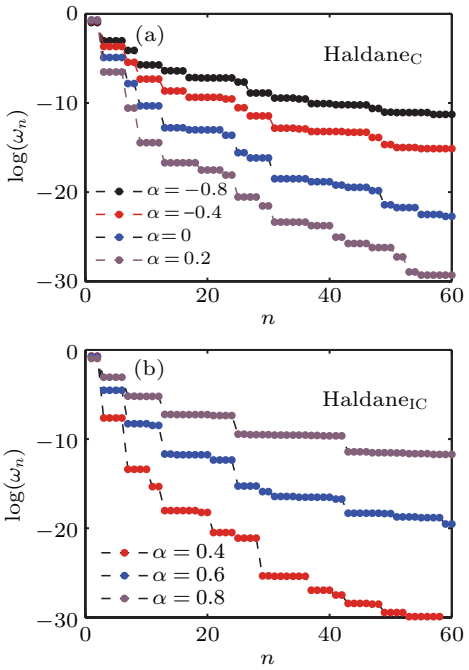


Fig. 2. Entanglement spectrum E_n as a function of n for (a) Haldane$_{\rm C}$ phase and (b) Haldane$_{\rm IC}$ phase for different α parameters. The number of dots on each level indicates its degeneracy. The bond dimension $\chi = 200$.

The topological phases can be characterized by the entanglement spectrum.[33–36] The entanglement spectrum of a pure state of a bipartite system is the full set of eigenvalues of the reduced density matrix obtained from tracing out one part. In several cases, the spectrum contains additional information besides the entanglement entropy. In numerical studies, the entanglement spectrum is a robust tool for identifying topological phases. For a bipartite system, the entanglement spectrum[37] is defined as follows:

$$E_n = -\log \omega_n, \tag{3}$$

where $\omega_n = \lambda_n^2$ denotes an eigenvalue of the reduced density matrix ρ, n is the number of largest eigenvalues kept. In Fig. 2, we plot the entanglement spectrum E_n as a function of n for (a) the Haldane$_{\rm C}$ phase with $\alpha = -0.8, -0.4, 0, 0.2$ and (b) the Haldane$_{\rm IC}$ phase with $\alpha = 0.4, 0.6, 0.8$. Here, the bond dimension $\chi = 200$. The results indicate that the entanglement spectrum shows double degeneracy in both phases. This means that the Haldane is a topological phase. But the entanglement spectrum can not distinguish the Haldane$_{\rm C}$ and Haldane$_{\rm IC}$ phases.

3. The bond-centered inversion nonlocal order parameter

The Haldane phase[2] is a typical example of the SPT phase,[29–31] which is protected by any of the following three symmetries: bond-centered inversion symmetry, time-reversal symmetry, and a dihedral group comprising any pair of π-rotations in the spin space.[29,30] The topological phase cannot be characterized by a local order parameter, which falls beyond the Landau paradigm, but can be characterized by nonlocal order. The iMPS[32] and infinite density matrix renormalization group (iDMRG)[38] are robust tensor network algorithms, which can be exploited to efficiently simulate one-dimensional quantum many-body systems. The algorithms generate a ground state wave function in an iMPS representation and provide an efficient means to evaluate various physical observables. From the iMPS simulation, the ground state $|\psi\rangle$ is obtained, which is invariant under the two-site translation. In terms of the bond-centered inversion $I_{(1,L)}$, the bond-centered nonlocal order parameter for the segment comprising L bonds of type A–B is defined as follows:[39,40]

$$O = \frac{\langle\psi|I_{(1,L)}|\psi\rangle}{{\rm Tr}(\lambda_{\rm B}^4)}, \tag{4}$$

where $\lambda_{\rm B}$ denotes the Schmidt decomposition coefficient, and the segment length L is even. A graphical representation is shown in Fig. 3.

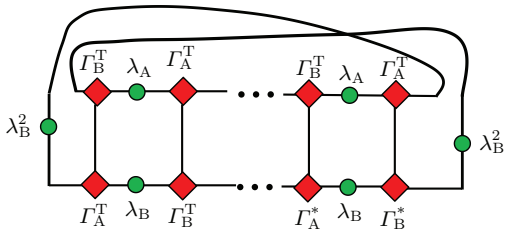


Fig. 3. Graphical representation of nonlocal order parameters in the MPS picture for the segment comprising L bonds of type A–B.

We plot the nonlocal order parameter O as a function of α with the bond dimension $\chi = 200$ in the Haldane phase in Fig. 4(a). In the entire Haldane phase, O reaches a saturation value of -1 when α is away from the quantum phase points ± 1, indicating that the nonlocal order parameter O cannot distinguish between the Haldane$_{\rm C}$ and Haldane$_{\rm IC}$ phases, but can be used to characterize the SPT phase. In addition, we plot the nonlocal order parameter O as a function of the segment

length L with the bond dimension $\chi = 200$ for $\alpha = -0.4, 0, 0.4$ [Fig. 4(b)]. This indicates that the nonlocal order parameter O tends to a saturation value of -1 as the segment length L increases.

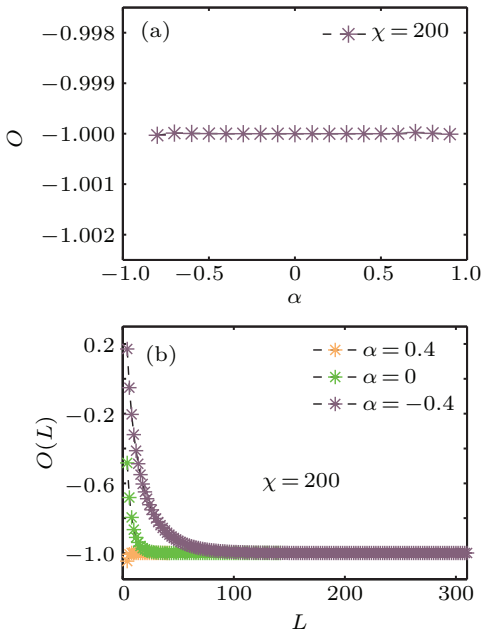


Fig. 4. (a) Nonlocal order parameter O as a function of α with the bond dimension $\chi = 200$ in the Haldane phase. (b) Saturation of the nonlocal order parameter O, with the block size L being even, for $\alpha = -0.4$, 0, 0.4.

4. String order parameter

In the Haldane phase for the spin-1 BLBQ model with $-1 < \alpha < 1$, due to the hidden $Z_2 \times Z_2$ symmetry is broken,[41] the characteristic order can be measured by the string correlation function[42]

$$g(r) = \langle S_i^z \exp\left[\mathrm{i}\pi \sum_{k=i+1}^{j-1} S_k^z\right] S_j^z \rangle, \tag{5}$$

where $r = |i - j|$ denotes the lattice distance. In Fig. 5, we plot the string correlation function $g(r)$ as a function of the lattice distance r for (a) Haldane$_{\mathrm{C}}$ phase with $\alpha = -0.8$, -0.4, 0, 0.2 and (b) Haldane$_{\mathrm{IC}}$ phase with $\alpha = 0.4$, 0.6, 0.8. Here, the bond dimension $\chi = 200$. For a small lattice distance r, the $g(r)$ rapidly tends to a saturation value, indicating that the long-range order is evident. If we continue to increase the lattice distance r, the saturation value of string correlation $g(r)$ stays at the limiting value. For $\alpha = 0$, the spin-1 BLBQ model corresponds to the spin-1 antiferromagnetic Heisenberg model. Consequently, we compute the string correlation function, which shows a long-range order with $g(\infty) = -0.374324443$, with the bond dimension $\chi = 200$. Our result agrees with the result $g(\infty) = -0.374325096(2)$ from the iDMRG algorithm.[43] The behaviors of string correlation are the same in both the Haldane$_{\mathrm{C}}$ and Haldane$_{\mathrm{IC}}$ phases. Note our results show that the entanglement spectrum, the bond-centered inversion nonlocal order parameter, and the string correlation cannot distinguish the Haldane$_{\mathrm{C}}$–Haldane$_{\mathrm{IC}}$ transition, but they can clearly characterize the Haldane phase.

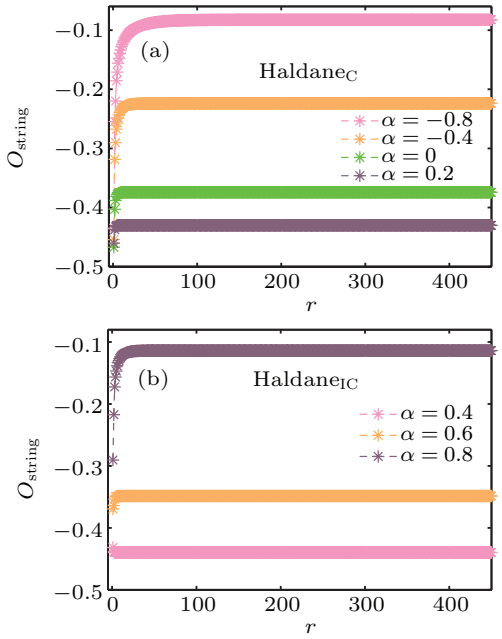


Fig. 5. String correlation function $g(r)$ as a function of the lattice distance r for (a) Haldane$_{\mathrm{C}}$ phase and (b) Haldane$_{\mathrm{IC}}$ phase for different α parameters. The bond dimension $\chi = 200$.

5. Characterization of the Haldane$_{\mathrm{C}}$ and Haldane$_{\mathrm{IC}}$ phases

We now characterize the Haldane$_{\mathrm{C}}$ and Haldane$_{\mathrm{IC}}$ phases. Physically, "incommensurate" means the wavelength of the oscillation pattern is not an integer multiple of the lattice spacing. To characterize the Haldane$_{\mathrm{C}}$ and Haldane$_{\mathrm{IC}}$ phases, we calculate the transversal spin correlation $C(r) = \langle \boldsymbol{S}_i^+ \boldsymbol{S}_j^- \rangle$ with the spin operator $\boldsymbol{S}^{\pm} = S^x \pm \mathrm{i} S^y$. By a Fourier transform, the static spin structure factor of the transversal spin correlation is defined as follows:[44–46]

$$S^{+-}(\boldsymbol{q}) = \sum_j \mathrm{e}^{-\mathrm{i}\boldsymbol{q}\cdot(r_0 - r_j)} \langle \boldsymbol{S}_0^+ \boldsymbol{S}_j^- \rangle. \tag{6}$$

In Fig. 6(a), we plot the transversal spin correlation $C(r)$ in the Haldane$_{\mathrm{C}}$ phase (up) with $\alpha = -0.8$, -0.4, 0, 0.2 and the Haldane$_{\mathrm{IC}}$ phase (down) with $\alpha = 0.4$, 0.6, 0.8. The transversal spin correlation tends to zero as the lattice distance r increases, indicating that no off-diagonal order exists in the Haldane phase. In addition, Fig. 6(a) clearly shows that the transversal spin correlation $\langle \boldsymbol{S}_i^+ \boldsymbol{S}_j^- \rangle$ takes on different forms of decay in both Haldane$_{\mathrm{C}}$ and Haldane$_{\mathrm{IC}}$ phases. To obtain the decay function, as an illustrative example, we choose two typical ground states in the Haldane$_{\mathrm{C}}$ and Haldane$_{\mathrm{IC}}$ phases. In Fig. 6(b) (up), for small lattice distance $r = 100$, a number fit to the transversal spin correlation $\langle \boldsymbol{S}_i^+ \boldsymbol{S}_j^- \rangle$ (for odd lattice distance) is performed with $\alpha = -0.8$ in the Haldane$_{\mathrm{C}}$,

with the fitting function $C(r) = ar^{-\eta} + b$. The numerical constants are given as $\eta = 0.5118$, $a = 0.69$, and $b = -0.0278$. In Fig. 6(b) (down), for the small lattice distance $r = 30$, a number fit to the transversal spin correlation $\langle \boldsymbol{S}_i^+ \boldsymbol{S}_j^- \rangle$ is performed with $\alpha = 0.6$ in the Haldane$_{\rm IC}$, with the fitting function $C(r) = r^{-\eta}\cos(qr) + c$ and $q = \beta\pi$. The numerical constants are given as $\eta = 1.533$, $\beta = 1.264$, and $c = -0.0012$. The solid black line is the fit. Our results clearly show that the dominant decaying form to the transversal spin correlation is $\propto r^{-\eta}$ for the Haldane$_{\rm C}$ phase and $\propto r^{-\eta}\cos(qr)$ for the Haldane$_{\rm IC}$ phase for small lattice distance r. In addition, to further characterize the Haldane$_{\rm C}$ and Haldane$_{\rm IC}$ phases, we investigate the momentum distribution of the spin structure factor $S^{+-}(q)$. In Fig. 6(c) (up), we plot the corresponding momentum distribution of the spin structure factor $S^{+-}(q)$ in the Haldane$_{\rm C}$ phase with $\alpha = -0.8$, -0.4, 0, 0.2. For Haldane$_{\rm C}$ phase, we observe that the peaks for the transversal spin structure factor $S^{+-}(q)$ at $q = \pm\pi$ are the uniform background. In Fig. 6(c) (down), we plot the corresponding momentum distribution of the spin structure factor $S^{+-}(q)$ in the Haldane$_{\rm IC}$ phase with $\alpha = 0.4, 0.6, 0.8$. For Haldane$_{\rm IC}$ phase, we observe that the dips for the transversal spin structure factor $S^{+-}(q)$ are located at $q = \pm\pi$. In addition, we do see some peaks around (i) $q = \pm 0.7\pi$, $\pm 1.3\pi$ for $\alpha = 0.8$, (ii) $q = \pm 0.66\pi$, $\pm 1.34\pi$ for $\alpha = 0.6$ and (iii) $q = \pm 0.78\pi$, $\pm 1.22\pi$ for $\alpha = 0.4$ in the transversal spin structure factor $S^{+-}(q)$, which account for the incommensurate contribution. Here, the bond dimension is $\chi = 200$.

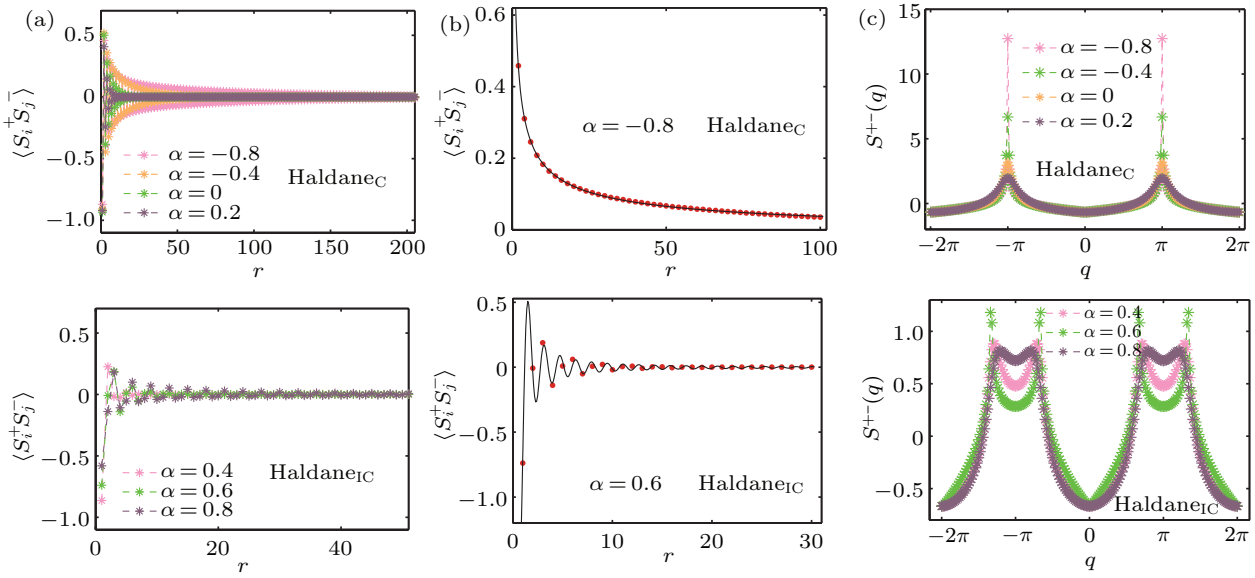


Fig. 6. (a) Transversal spin correlation $C(r)$ in the Haldane$_{\rm C}$ phase (up) and the Haldane$_{\rm IC}$ phase (down) for various α parameters, (b) the fitting of the transversal correlation $C(r)$ in the Haldane$_{\rm C}$ phase (up) with $\alpha = -0.8$ and the Haldane$_{\rm IC}$ phase (down) with $\alpha = 0.6$, and (c) the corresponding momentum distribution of the structure factor $S^{+-}(q)$ in the Haldane$_{\rm C}$ phase (up) and the Haldane$_{\rm IC}$ phase (down) for various α parameters. The bond dimension $\chi = 200$.

As a result, the transversal spin correlation $\langle \boldsymbol{S}_i^+ \boldsymbol{S}_j^- \rangle$ exhibits different decay behaviors in Haldane$_{\rm C}$ and Haldane$_{\rm IC}$ phases, respectively. The dominant decaying form of the transversal spin correlation $\langle \boldsymbol{S}_i^+ \boldsymbol{S}_j^- \rangle$ is proportional to $r^{-\eta}$ in the Haldane$_{\rm C}$ phase and is proportional to $r^{-\eta}\cos(qr)$ in the Haldane$_{\rm IC}$ phase. In addition, the transversal spin structure factor $S^{+-}(q)$ exhibits an incommensurate oscillation pattern in the Haldane$_{\rm IC}$.

6. Summary

The Haldane$_C$ and Haldane$_{\rm IC}$ phases for the spin-1 BLBQ model are investigated using the iMPS algorithm. A phase transition point, which corresponds to the AKLT point with $\alpha = 1/3$, is located by the bipartite entanglement entropy between the Haldane$_{\rm C}$ and Haldane$_{\rm IC}$ phases. In both phases, the entanglement spectrum shows double degeneracy. We calculate the nonlocal order parameter of the bond-centered inversion in both phases, which rapidly approaches a saturation value of -1 as the segment length L increases. The nonlocal string order is also calculated; a nonzero value string order can be used to characterize the topological phases. For $\alpha = 0$, the spin-1 BLBQ model corresponds to the spin-1 antiferromagnetic Heisenberg model, and the string correlation function shows long-range order, with $g(\infty) \cong -0.374325096(2)$ from the iDMRG algorithm.[43] Our results agree with the results from the iDMRG algorithm.[43] In addition, to distinguish the Haldane$_C$ and Haldane$_{\rm IC}$ phases, the transversal spin correlation $\langle \boldsymbol{S}_i^+ \boldsymbol{S}_j^- \rangle$ and corresponding momentum distribution of the structure factor $S^{+-}(q)$ are analyzed. Our results show that the dominant decaying form of the transversal spin correlation is proportional to $r^{-\eta}$ for Haldane$_{\rm C}$ phase and is proportional to $r^{-\eta}\cos(qr)$ for Haldane$_{\rm IC}$ phase for a small lattice distance

r. In addition, the Haldane$_{\rm IC}$ phase exhibits an incommensurate oscillation pattern in the spin correlation structure factor.

Acknowledgements

Project supported by the National Natural Science Foundation of China (Grant No. 11805285), the Natural Science Foundation of Shaanxi Province of China (Grant No. 2022JM-033), and the Science and Technology Research Program of Chongqing Municipal Education Commission (Grant No. KJQN 201900703).

References

[1] Sachdev S 1999 *Quantum Phase Transitions* (Cambridge University Press, Cambridge)
[2] Haldane F D M 1983 *Phys. Rev. Lett.* **50** 1153
[3] Haldane F D M 1983 *Phys. Lett. A* **93** 464
[4] Murashima T and Nomura K 2006 *Phys. Rev. B* **73** 214431
[5] Fáth G and Sütõ A 2000 *Phys. Rev. B* **62** 3778
[6] Nomura K 2003 *J. Phys. Soc. Jpn.* **72** 476
[7] Yarotsky D A 2008 *J. Stat. Phys.* **130** 957
[8] Chubukov A V 1991 *Phys. Rev. B* **43** 3337
[9] Kawashima N 2002 *Prog. Theor. Phys. Suppl.* **145** 138
[10] Ivanov B A and Kolezhuk A K 2003 *Phys. Rev. B* **68** 052401
[11] Buchta K, Fáth G, Legeza O and Sólyom J 2005 *Phys. Rev. B* **72** 054433
[12] Rizzi M, Rossini D, De Chiara G, Montangero S and Fazio R 2005 *Phys. Rev. Lett.* **95** 240404
[13] Läuchli A, Schmid G and Trebst S 2006 *Phys. Rev. B* **74** 144426
[14] Porras D, Verstraete F and Cirac J I 2006 *Phys. Rev. B* **73** 014410
[15] Romero-Isart O, Eckert K and Sanpera A 2007 *Phys. Rev. A* **75** 050303
[16] Dai Y W, Shi Q Q, Zhou H Q and McCulloch I 2022 arXiv: 2201.01434
[17] Chen A M, Su Y H and Wang H L 2015 *Eur. Phys. J. B* **88** 269
[18] Jakab D, Szirmai G and Zimborás Z 2018 *J. Phys. A: Math. Theor.* **51** 105201
[19] Li P and Kou S P 2012 *J. Phys.: Condens. Matter* **24** 446001
[20] Fáth G and Sólyom J 1991 *Phys. Rev. B* **44** 11836
[21] Sutherland B 1975 *Phys. Rev. B* **12** 3795
[22] Batista C D, Ortiz G and Gubernatis J E 2002 *Phys. Rev. B* **65** 180402
[23] Affleck I 1990 *J. Phys.: Condens. Matter* **2** 405
[24] Takhtajan L 1982 *Phys. Lett. A* **87** 479
[25] Babujian H 1983 *Nucl. Phys. B* **215** 317
[26] Barber M N and Batchelor M T 1989 *Phys. Rev. B* **40** 4621
[27] Affeck T, Kennedy T, Lieb E and Tasaki H 1987 *Phys. Rev. Lett.* **59** 799
[28] Pollmann F, Turner A M, Berg E and Oshikawa M 2010 *Phys. Rev. B* **81** 064439
[29] Chen X, Gu Z C and Wen X G 2011 *Phys. Rev. B* **83** 035107
[30] Pollmann F, Turner A M, Berg E and Oshikawa M 2010 *Phys. Rev. B* **81** 064439
[31] Rao W J, Zhu G Y and Zhang G M 2016 *Phys. Rev. B* **93** 165135
[32] Vidal G 2007 *Phys. Rev. Lett.* **98** 070201
[33] Li H and Haldane F D M 2008 *Phys. Rev. Lett.* **101** 010504
[34] Levin M and Wen X G 2006 *Phys. Rev. Lett.* **96** 110405
[35] Kitaev A and Preskill J 2006 *Phys. Rev. Lett.* **96** 110404
[36] Pollmann F and Turner A M 2010 *Phys. Rev. B* **81** 064439
[37] Calabrese P and Lefevre A 2008 *Phys. Rev. A* **78** 032329
[38] McCulloch I P 2008 arXiv: 0804.2509
[39] Pollmann F and Turner A M 2012 *Phys. Rev. B* **86** 125441
[40] Fuji Y, Pollmann F and Oshikawa M 2015 *Phys. Rev. Lett.* **114** 177204
[41] Kennedy T and Tasaki H 1992 *Phys. Rev. B* **45** 304
[42] Tu H H, Zhang G M and Xiang T 2008 *J. Phys. A: Math. Theor.* **41** 415201
[43] White S R and Huse D A 1993 *Phys. Rev. B* **48** 3844
[44] Sengupta P and Batista C D 2007 *Phys. Rev. Lett.* **98** 227201
[45] Zare M H and Mosadeq H 2021 *Phys. Rev. B* **104** 115154
[46] Dai Y W, Liu X J, Li S H and Chen A M 2022 *Phys. Rev. E* **106** 054104